Atmospheric Research 205 (2018) 48–59

Contents lists available at ScienceDirect

Atmospheric Research

journal homepage: www.elsevier.com/locate/atmosres

Discriminating the precipitation phase based on different temperature thresholds in the Songhua River Basin, China

Keyuan Zhong[a], Fenli Zheng[a,b,*], Ximeng Xu[a], Chao Qin[a]

[a] Institute of Soil and Water Conservation, State Key Laboratory of Soil Erosion and Dryland Farming on the Loess Plateau, Northwest A&F University, No. 26 Xinong Rd., Yangling, 712100, Shaanxi, PR China

[b] Institute of Soil and Water Conservation, CAS & MWR, No. 26 Xinong Rd., Yangling, 712100, Shaanxi, PR China

ARTICLE INFO

Keywords:
Precipitation phase
Threshold temperature
Snowfall
Hydrologic process
Hydrological model
The Songhua River Basin

ABSTRACT

Different precipitation phases (rain, snow or sleet) differ greatly in their hydrological and erosional processes. Therefore, accurate discrimination of the precipitation phase is highly important when researching hydrologic processes and climate change at high latitudes and mountainous regions. The objective of this study was to identify suitable temperature thresholds for discriminating the precipitation phase in the Songhua River Basin (SRB) based on 20-year daily precipitation collected from 60 meteorological stations located in and around the basin. Two methods, the air temperature method (AT method) and the wet bulb temperature method (WBT method), were used to discriminate the precipitation phase. Thirteen temperature thresholds were used to discriminate snowfall in the SRB. These thresholds included air temperatures from 0 to 5.5 °C at intervals of 0.5 °C and the wet bulb temperature (WBT). Three evaluation indices, the error percentage of discriminated snowfall days (*Ep*), the relative error of discriminated snowfall (*Re*) and the determination coefficient (R^2), were applied to assess the discrimination accuracy. The results showed that 2.5 °C was the optimum threshold temperature for discriminating snowfall at the scale of the entire basin. Due to differences in the landscape conditions at the different stations, the optimum threshold varied by station. The optimal threshold ranged 1.5–4.0 °C, and 19 stations, 17 stations and 18 stations had optimal thresholds of 2.5 °C, 3.0 °C, and 3.5 °C respectively, occupying 90% of all stations. Compared with using a single suitable temperature threshold to discriminate snowfall throughout the basin, it was more accurate to use the optimum threshold at each station to estimate snowfall in the basin. In addition, snowfall was underestimated when the temperature threshold was the WBT and when the temperature threshold was below 2.5 °C, whereas snowfall was overestimated when the temperature threshold exceeded 4.0 °C at most stations. The results of this study provide information for climate change research and hydrological process simulations in the SRB, as well as provide reference information for discriminating precipitation phase in other regions.

1. Introduction

Precipitation is one of the most important components of the water and energy cycles on land surfaces, and changes in the precipitation phase (rain, snow or sleet) significantly impact water and energy balances (Ding et al., 2014). Rainfall-runoff and snow melting processes vary greatly in hydrology (Ding et al., 2014). In general, surface runoff produced by rainfall directly runs into rivers and takes part in water and energy cycles, whereas snowfall accumulates on the Earth's surface, melts and infiltrates into the soil at a certain temperature. When snowfall accumulates on the Earth's surface, it significantly increases the surface albedo and affects the energy balance at the land surface (Hock, 2003; Chen et al., 2014). At remote meteorological stations, automatic observation stations and some manual observation stations, the precipitation phase is unobtainable. However, some fields are strongly dependent on accurate precipitation phase records, such as hydrological process research and weather forecasting. Therefore, it is very important to determine the precipitation phase when researching hydrological processes and climate change (Chen et al., 2014).

Many researches quantified the discrimination of the precipitation phase in different regions. These studies can be summarized as three types. The first type discriminates the precipitation phase based on vertical atmospheric conditions, such as the vertical temperature, atmospheric pressure and freezing level height (Czys et al., 1996; Rauber et al., 2001; Lundquist et al., 2008). This method is based on the physical mechanisms to discriminate the precipitation phase, which are

* Corresponding author at: Institute of Soil and Water Conservation, Northwest A&F University, 26 Xinong Rd., Yangling, 712100, Shaanxi, PR China.
E-mail address: flzh@ms.iswc.ac.cn (F. Zheng).

https://doi.org/10.1016/j.atmosres.2018.02.002
Received 4 August 2017; Received in revised form 29 November 2017; Accepted 6 February 2018
Available online 07 February 2018
0169-8095/ © 2018 Elsevier B.V. All rights reserved.

highly accurate, and widely used in weather forecasting. Because vertical atmospheric data are difficult to obtain and mainly applicable to short-term forecasts, they have had limited use in discriminating the long-term precipitation phase. The second type discriminates the precipitation phase based on remote sensing technologies, such as weather radar and satellite images, which have shown many advantages for identifying snow and rain (Fassnacht et al., 2001; Han et al., 2010; Ding et al., 2014). However, these technologies are restricted by terrain and have poor accuracy at high altitudes and complex mountainous regions (Fassnacht et al., 2001; Maurer and Mass, 2006). The third type discriminates the precipitation phase based on surface atmospheric and landscape conditions, such as the surface air temperature, dew point temperature, relative humidity, elevation and wet bulb temperature (Fassnacht et al., 2001; Habets et al., 2008). Because these data are easily obtained and have acceptable accuracy, this is the most commonly used method for estimating the precipitation phase (Chen et al., 2014; Ding et al., 2014; Liu et al., 2016).

Among the surface atmospheric and landscape conditions used to estimate the precipitation phase, surface temperature is the most widely used indicator to discriminate precipitation phase (Habets et al., 2008). Currently, most hydrological models use this method to identify the precipitation phase. Notably, this method is used in the SWAT (Soil and Water Assessment Tool, Arnold et al., 1994), HBV model (Hydrologiska Byråns Vattenbalansavdelning, Bergström, 1992) and AnnAGNPS model (Annualized Agricultural Nonpoint Source, Bingner et al., 2003). Chen et al. (2014) found that the surface air temperature method (AT method) performed better than the wet bulb temperature method (WBT method) when the critical air temperature was 2 °C. They also found that the optimum threshold temperature for discriminating the precipitation phase differed in different terrains, and threshold temperatures were higher at higher elevation. Dai (2008) demonstrated that differences in temperature and pressure altered the freezing point in oceans and on land and affected the temperature thresholds of two different landscape conditions. Small-scale differences in terrain can affect the solar heating of the ground, orographic lifting and cold air drainage, which subsequently affects the threshold temperature (Rajagopal and Harpold, 2016). Ding et al. (2014) concluded that relative humidity, elevation and air temperature affected the precipitation phase and proposed that the wet bulb temperature could be used to identify precipitation phases in China. Dew point temperature and relative humidity have also been applied to identify phases of precipitation (Harpold et al., 2017; Thériault et al., 2006). Kienzle (2008) found that precipitation phases were highly dependent on the landscape condition, and some researchers have developed empirical models to determine precipitation phase based on specific ground-surface conditions (Bourgouin, 2000; Feiccabrino and Lundberg, 2008; Marks et al., 2013; Liu et al., 2016; Rajagopal and Harpold, 2016). These studies discriminated precipitation phases in different regions through various methods and provided useful information for estimating precipitation phases in different regions.

Due to differences in the atmospheric and landscape conditions, the threshold temperatures used to discriminate the precipitation phase vary and require further research in specific regions. The Songhua River Basin (SRB) is one of the main regions of snowfall and snow cover in China (Qin et al., 2006). The average annual snowfall (snow water equivalent) in the basin is between 30 and 150 mm and accounts for 7%–25% of the annual precipitation (Jiao et al., 2009; Yang, 2015). Snow melts and converges into rivers, forming spring floods from April to May. Snowmelt runoff accounts for 10%–15% of the discharge in the basin (Yang, 2015) and contributes to 5.8%–27.7% of sediment loads in the basin (Jiao et al., 2009). The SRB is also one of the most sensitive regions to climate warming in China (Jiao et al., 2009; Song et al., 2015). The increasing rate of mean annual temperature was 0.33 °C/decade from 1960 to 2014 (Zhong et al., 2017), and this increase trend was higher than the mean trend in China (0.25 °C/decade). With the increase in temperature, some snowfall may shift to rainfall, which may greatly affect the hydrologic processes and water cycle in this basin. In addition, due to the increasing effects of human activities and climate change, soil erosion has become very serious in the basin (An et al., 2014; Yang et al., 2016). Scholars have attempted to simulate hydrologic and erosion processes using hydrological models and have taken measures to protect the soil and water resources in the basin (Feng et al., 2013; Zhang et al., 2012). However, at present, long-term precipitation phase observational records are lacking (without specific precipitation phases after 1979) in China (Wang et al., 2016). These data gaps greatly affect the accuracy of hydrologic process simulations and limit the understanding of snowfall and climate changes (Chen et al., 2014; Liu et al., 2016).

The objective of this study was to detect suitable temperature thresholds for separating snowfall from precipitation in the SRB based on observation data collected from 60 meteorological stations within and around the basin between 1960 and 1979. The results will enrich studies of discriminated precipitation phase in different regions and provide information for climate change research and hydrological process simulations in the SRB, as well as provide reference information for discriminating precipitation phases in other regions.

2. Materials and methods

2.1. Study area and data sources

2.1.1. Study area

The SRB is located in northeastern China. It has an area of 546,000 km^2 and stretches latitudinally from 41°42′ N to 51°38′ N and longitudinally from 119°52′ E to 132°31′ E (Fig. 1). The basin is located in a temperate climate zone, and the annual mean temperature ranges from 3 °C to 5 °C (Qi and Fan, 2015). The lowest temperature was −50.2 °C, which was recorded in 1966. Annual precipitation in the basin ranged from 397.8 mm to 684.8 mm during the period 1960–2014 (Zhong and Zheng, 2017), and precipitation decreases from the southeast to the north and west.

The terrain in the SRB greatly varies, which is dominated by plains and hills. The Changbai Mountains are located in the east, and the Greater Khingan Mountains are located in the west. The two ranges contain the headwaters of the Second Songhua River and the Nenjiang, respectively. These two tributaries merge into the Songhua River at the Sanjiang estuary. The Central Plain is located in the central part of the basin. Mollisol is the dominant soil type in the SRB, which contains 60% of the black soil in China by area. The SRB is a primary grain-producing region and commodity grain base for China. It is also one of the most sensitive regions to climate warming in China (Song et al., 2015; Zhong et al., 2017).

2.1.2. Data sources and quality control

The data used in this study were collected from 73 meteorological stations in northeast China and were provided by the Meteorological Information Center of the China Meteorological Administration (http://www.cma.gov.cn/2011qxfw/2011qsjgx/). The meteorological data have been maintained according to the World Meteorological Organization's (WMO) standards and the China Meteorological Administration's technical regulations regarding weather observations. This dataset has undergone strict quality control procedures (e.g., extreme value and time consistency tests) and has been widely used in studies of climatic change in China (Ding et al., 2014; Liu et al., 2016; Guan et al., 2017; Zhong et al., 2017).

In this database, snowfall events were labelled as 31XXX (XXX is the snow water equivalent) and snow and rainfall (sleet) events were labelled as 30XXX (Wang et al., 2016). The precipitation phase record spans from 1960 to 1979, and precipitation phase was not noted in the database after 1979. The database also contains daily mean, maximum and minimum temperatures; daily mean pressure; and daily mean relative humidity.

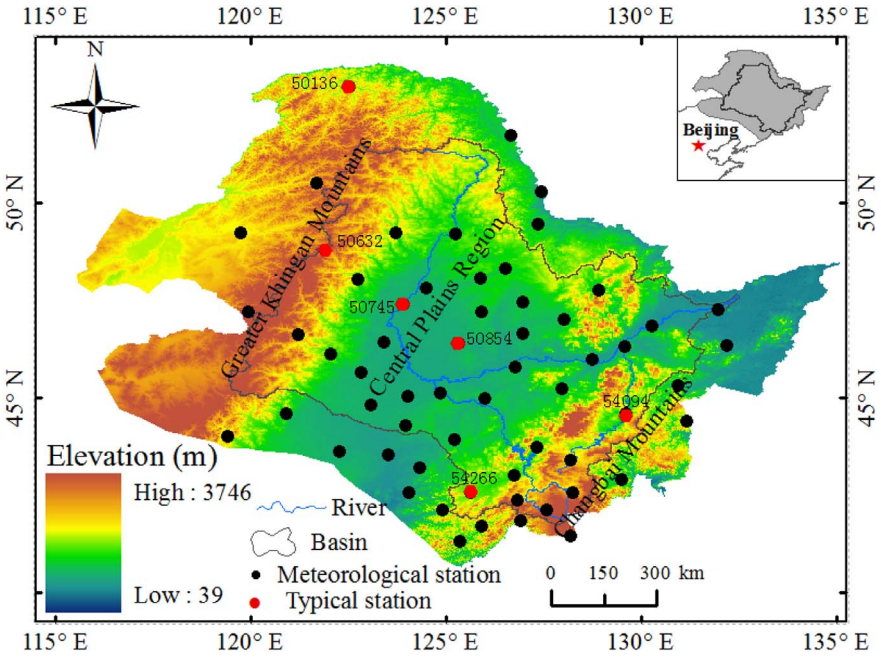

Fig. 1. Study area and distribution of the meteorological stations.

Due to the inconsistencies at early observation dates, shifting station locations and other reasons, some data were unrecorded at some meteorological stations. In this study, when unrecorded data exceeded 10% or continuously unrecorded data exceeded 30 d, the corresponding meteorological station was excluded (Zhong et al., 2017). Moreover, abnormal precipitation records, which included precipitation phases recorded as snow when the temperature was greater than or equal to 8 °C and recorded as rainfall when the temperature was below −3 °C, were ignored in this study (Auer, 1974; Feiccabrino et al., 2013; Ding et al., 2014; Liu et al., 2016). Finally, 60 complete stations in the SRB from 1960 to 1979 were selected. The data used in this study include daily precipitation, daily mean temperature, daily average pressure, daily average relative humidity and the elevation of each station. In addition, since the raw snowfall data is measured as the snow water equivalent, the snowfall mentioned hereinafter is the snow water equivalent (SWE, mm).

2.1.3. The choice of typical meteorological stations

The terrain in the SRB varies greatly (Fig. 1), which includes the Eastern Mountainous Hilly Region, Central Plains Region and Western Mountain Areas from east to west. The amount of snowfall is higher in mountainous regions and the southeastern part of the basin, while lower in the central part of the basin (Jiao et al., 2009). In this paper, some stations with different terrain and snowfall characteristics were chosen as typical meteorological stations to verify the discrimination accuracy. Stations 50136, 50745 and 54266 were located in different terrains and received different quantities of snowfall. These stations are shown along a line from northwest to southeast in Fig. 1. Additionally, stations 50632, 50854 and 54094 were located in different terrains along a line from west to east. The analysis of the discriminated accuracy of those stations can be used to illustrate the discrimination results at specific stations.

2.2. Methods

2.2.1. Air temperature method

The AT method discriminates the precipitation phase using a specific critical temperature; snowfall occurs when the temperature falls below the critical temperature (Liu et al., 2016), and rainfall occurs when the temperature exceeds the critical temperature (Formula (1)). The AT method contains single threshold and double threshold methods. Han et al. (2010) found that single thresholds yielded higher accuracies than double thresholds in most regions of China and that double thresholds was only suitable for some dry regions in China. Thus, in this study, the single threshold temperature method was used to discriminate snowfall, and 12 temperature thresholds from 0 to 5.5 °C at intervals of 0.5 °C were used to determine the suitable temperature thresholds.

$$P_S = \begin{cases} P & T \le T_o \\ 0 & T > T_o \end{cases} \quad (1)$$

P is the recorded daily precipitation (mm), T is the daily mean air temperature (°C), T_o is the critical threshold temperature (°C), and Ps is the discriminated snowfall (mm).

2.2.2. Wet bulb temperature method

The WBT method is similar to the AT method but also considers the effects of relative humidity, air pressure and elevation on the precipitation phase (Chen et al., 2014). Ding et al. (2014) developed a WBT method to discriminate the precipitation phase and proposed that it was a better indicator than the air temperature in China. Hence, that method was used in this study. To distinguish snowfall from precipitation, the algorithm used in this study was simplified, which did not consider sleet (Formula (2)). The formulae used to discriminate snowfall from precipitation are as follows:

$$P_S = \begin{cases} P & T_W \le T_A \\ 0 & T_W > T_A \end{cases}, \quad (2)$$

where P_s is the discriminated daily snowfall (mm), P is daily precipitation (mm), T_W is the wet bulb temperature (°C), and T_A is the threshold temperature (°C). T_W contains air temperature, pressure and humidity information, and its calculation is given in the Appendix A. T_A can be calculated as follows:

$$T_A = \begin{cases} 2\,T_0 - T_B & \frac{\Delta T}{\Delta S} > \ln 2 \\ T_0 & \frac{\Delta T}{\Delta S} \le \ln 2 \end{cases}. \quad (3)$$

Additionally, T_B, ΔT, ΔS and T_o can be calculated using the following equations:

$$T_B = \begin{cases} T_o - \Delta S \cdot \ln(e^{\Delta T/\Delta S} - 2 \cdot e^{-\Delta T/\Delta S}) & \frac{\Delta T}{\Delta S} > \ln 2 \\ T_o & \frac{\Delta T}{\Delta S} \le \ln 2 \end{cases}, \quad (4)$$

$$\Delta T = 0.215 - 0.099RH + 1.02RH^2, \quad (5)$$

$$\Delta S = 2.37 - 1.63RH, \quad (6)$$

and

$$T_o = -5.87 - 0.1Z + 0.09Z^2 + 16.6RH - 9.61RH^2, \quad (7)$$

where RH is daily mean relative humidity, which ranges from 0 to 1, and Z is elevation (km).

2.3. Evaluation indices of the discrimination accuracy

Three evaluation indices were used to evaluate the snowfall discrimination accuracy: the error percentage of discriminated snowfall days (Ep, %), relative error of discriminated snowfall (Re, %) and determination coefficient (R^2). Ep reflects the percentage of misclassified snowfall days to actual observed snowfall days (Formula (8)); misclassified snowfall days contain the number of snowfall days misclassified as rainfall days and the number of rainfall days misclassified as snowfall days. Re reflects the percentage of discriminated snowfall to actual observed snowfall. $Re < 0\%$ indicates that the snowfall is underestimated, and $Re > 0\%$ indicates that the snowfall is overestimated (Formula (9)). R^2 is a common aggregative index and is very sensitive to high-value records (Kienzle, 2008) (Formula (10)). The three evaluation indices can be expressed as follows:

$$Ep = \frac{S_{s-r} + S_{r-s}}{S_d} \times 100\%, \quad (8)$$

where S_{s-r} is the number of snowfall days misclassified as rainfall days (d), S_{r-s} is the number of rainfall days misclassified as snowfall days (d), and S_d is the observed snowfall days (d).

$$Re = \frac{S_e - S_o}{S_o} \times 100\% \quad (9)$$

and

$$R^2 = \frac{[\sum_{i=1}^{n}(S_e - \overline{S_e})(S_o - \overline{S_o})]^2}{\sum_{i=1}^{n}(S_e - \overline{S_e})^2 \sum_{i=1}^{n}(S_o - \overline{S_o})^2} \quad (10)$$

where S_e and S_o are the discriminated snowfall (mm) and observed snowfall (mm), respectively.

$Ep < 10\%$ reflects high accuracy when discriminating snowfall days, and $|Re| < 10\%$ indicates good accuracy when discriminating snowfall. In the hydrological model, $R^2 > 0.5$ indicates high accuracy for runoff process simulation (Lin et al., 2015; Zhong et al., 2016). Due to the specificity of discriminating snowfall (when snowfall misclassified as rainfall, the value will be zero; when rainfall misclassified as snowfall, which maybe regard as a heavy snowfall event), and the change of R^2 in discriminating snowfall is more sensitive than that of runoff simulation, especially for heavy snow events. The changes of R^2 for different threshold temperatures at the 6 typical meteorological stations were analysed in this study. We found that when the top five snow events were misclassified, R^2 rapidly decreased from 0.5 to below 0.20 at the daily time steps, and similar conclusion were also presented by Rajagopal and Harpold (2016). Moreover, Liu et al. (2016) support this conclusion (high R^2 at annual time steps, and low R^2 at the daily time steps in discriminating snowfall). Therefore, the identification of heavy snowfall events is considered acceptable in this paper when $R^2 > 0.20$ at the daily time steps. When all three indices are consistent with the given criteria ($Ep < 10\%$, $|Re| < 10\%$ and $R^2 > 0.2$), the threshold temperatures can accurately discriminate snowfall at the stations.

The optimum threshold at each station was selected based on the following principles (Table 1). 1) When all three indices are consistent with the given criteria ($Ep < 10\%$, $|Re| < 10\%$ and $R^2 > 0.2$), the optimum threshold temperature is the threshold temperature with minimum Ep. 2) When all three indices are consistent with the given criteria ($Ep < 10\%$, $|Re| < 10\%$ and $R^2 > 0.2$) and the minimum Ep is observed at two threshold temperatures, the optimum threshold temperature is the threshold temperature with smaller Re in the two threshold temperatures (the threshold temperatures with minimum Ep). 3) When Ep and Re are consistent with the criteria ($Ep < 10\%$ and $|Re| < 10\%$) but $R^2 < 0.2$, the optimum threshold temperature is the threshold temperature with minimum Ep in which threshold temperature fulfilled with the Ep and Re. 4) When Ep and R^2 are consistent with the criteria ($Ep < 10\%$ and $R^2 > 0.2$) but $|Re| > 10\%$, the optimum threshold temperature is the threshold temperature with minimum Ep in which threshold temperature fulfilled with the Ep and R^2. 5) Other situations are similar to the above situations, but overall, Ep is the preferential index, Re is the secondary index, and R^2 is the supplementary index (Table 1).

3. Results

3.1. Snowfall profile in the SRB during the period 1960–1979

Fig. 2 shows the profile of snowfall in the SRB. The annual average snowfall was 52.09 mm, and annual average number of snowfall days was 32.73 d in the SRB during the period 1960–1979. The average duration of the snow season was 174.77 d. The average first snowfall date was October 21, and the last snowfall date was April 4. The snowfall quantity was high in the southeastern part of the basin and mountainous regions, and highest in the southeastern part of the basin (> 90 mm) (Fig. 2). The lowest amount of snowfall and least minimum of snowfall days occurred in the southern part of the Central Plain Region (< 45 mm and 27 d, respectively).

Fig. 3 shows the changes in snowfall and snowfall days with the temperature in the SRB during the period 1960–1979. The snowfall increased with increasing air temperature from −40 °C to 1 °C. The largest amount of snowfall, 86.5 mm, occurred at 0–1 °C (Fig. 3), then, snowfall decreased with the increasing of temperature when temperature above 1 °C. There was only 6.46 mm of snowfall at 7–8 °C during these 20 years. The snowfall days increased as the air temperature increased from −40 °C to −17 °C and remained high and fluctuated between −17 °C and 1 °C. The greatest number of snowfall days occurred at 0–1 °C (25.51 d) and rapidly diminished when temperature was above 1 °C. Only one snowfall day occurred at 7–8 °C over the past 20 years. Snowfall was mainly concentrated from −5 °C to 5 °C to and snowfall days were concentrated between −18 °C and 3 °C in the basin (Fig. 3).

3.2. Discriminating snowfall in the SRB

3.2.1. Discriminating snowfall in the SRB at the basin scale

Fig. 4 shows the changes in the mean Ep, Re and R^2 at 60 stations for different threshold temperatures in the SRB during the period 1960–1979. Ep decreased with increasing temperature, reached a trough of 8.79% at 2.5 °C and then increased with increasing temperature (Fig. 4a and Table 2). The Ep values at 2.0 °C, 2.5 °C, 3.0 °C, 3.5 °C and WBT were < 10%, which indicates good accuracy when discriminating snowfall days.

Re increased as the temperature threshold increased (Fig. 4b and Table 2), an increase from −34.47% at 0 °C to 28.75% at 5.5 °C. The smallest $|Re|$ occurred at 3.0 °C (−1.59%). The temperature thresholds, including 2.5 °C, 3.0 °C 3.5 °C and 4 °C, effectively discriminated snowfall quantity ($|Re| < 10\%$), with Re values of −6.66%, −1.59%, 3.85%, and 9.68%, respectively.

R^2 increased with increasing temperature threshold, reached a peak of 0.260 at 3.5 °C, and then slowly decreased with increasing temperature threshold (Fig. 4c and Table 2). When temperature threshold

Table 1
Principles of optimum threshold selection.

Situation	*Ep* (%)	*Re* (%)	R^2	optimal threshold
1	< 10	< 10	> 0.2	Min(*Ep*) for ($Ep < 10\% \cap |Re| < 10\% \cap R^2 > 0.2$)
2	< 10 < 10	< 10	> 0.2	Min (*Re*) for min(*Ep*) for ($Ep < 10\% \cap |Re| < 10\% \cap R^2 > 0.2$)
3	< 10	< 10	< 0.2	Min(*Ep*) for ($Ep < 10\% \cap |Re| < 10\%$)
4	< 10	> 10	> 0.2	Min(*Ep*) for ($Ep < 10\% \cap R^2 > 0.2$)
5	> 10	< 10	> 0.2	Min(*Ep*) for ($|Re| < 10\% \cap R^2 > 0.2$)
6	> 10	> 10	< 0.2	Min(*Ep*)

Note: Min(*Ep*) for ($Ep < 10\% \cap |Re| < 10\% \cap R^2 > 0.2$) indicates that when all three indices are consistent with the given criteria ($Ep < 10\%$, $|Re| < 10\%$ and $R^2 > 0.2$), the optimum threshold temperature is the threshold temperature of the smallest *Ep*. < 10 < 10 indicates that the minimum *Ep* was repeated for two threshold temperatures.

was between 3.0 °C and 4.5 °C, R^2 values were above 0.250 (Table 2). When the temperature threshold was equal to or > 2.0 °C (2.0 °C, 2.5 °C, 3.0 °C, 3.5 °C, 4.0 °C, 4.5 °C, 5.0 °C and 5.5 °C) and the WBT, the R^2 exceeded 0.20, indicating good effectiveness when discriminating heavy snowfall events.

An comprehensive consideration of the three indices ($Ep < 10\%$, $Re < 10\%$ and $R^2 > 0.2$) showed that temperature threshold of 2.5 °C, 3.0 °C, and 3.5 °C can be used to effectively identify snowfall events in the SRB. Based on the principle that *Ep* is the preferential index (Min (*Ep*) for ($Ep < 10\% \cap |Re| < 10\% \cap R^2 > 0.2$)), the threshold temperature with the smallest *Ep* determined the optimum threshold. Therefore, 2.5 °C was the optimum threshold of the 13 threshold temperatures at the basin scale (Fig. 4a and Table 2).

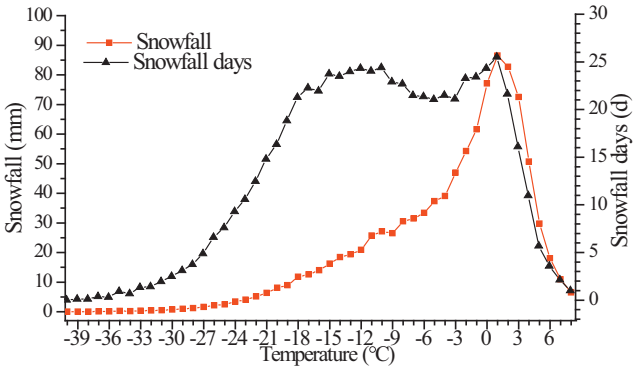

Fig. 3. Changes in snowfall and snowfall days with temperature in the SRB during the period 1960–1979.

3.2.2. Discrimination of snowfall at different stations

To further illustrate the discrimination results for each station, the number of stations that satisfied the requirements of the given evaluation indices ($Ep < 10\%$, $Re < 10\%$ and $R^2 > 0.2$) was counted (Fig. 5). The number of stations that fulfilled the *Ep* criterion ($Ep < 10\%$) increased with increasing temperature and reached a peak of 40 stations at 2.5 °C before decreasing as the temperature increased (Fig. 5a). The WBT had a number of stations that met the *Ep* criterion (39 stations), followed by 3 °C with 38 stations. Only two stations met the criterion of *Ep* values at 0 °C and 5.5 °C. Additionally, eleven stations did not pass the *Ep* criterion ($Ep < 10\%$) at any threshold temperature.

The number of stations that passed the relative error criterion ($Re < 10\%$) was similar to that for *Ep*; the number increased as the threshold temperature increased, reaching a peak at 3.5 °C with 51 stations and subsequently decreasing with increasing temperature (Fig. 5b). Forty-eight and 37 stations passed the *Re* criterion at 3 °C and 4 °C, respectively. Additionally, no stations passed the *Re* criterion ($Re < 10\%$) at 0 °C and 0.5 °C, as snowfall was underestimated.

However, the number of stations that passed the determination coefficient criterion ($R^2 > 0.20$) rapidly increased with increasing temperature, reaching a peak at 3.5 °C with 50 stations before slowly decreasing with temperature (Fig. 5c). The fewest number of stations (only 7 stations) passed the R^2 criterion at 0 °C. For WBT and all temperatures above 2.0 °C, > 32 stations passed the R^2 criterion.

Based on the analysis of the changes in the number of stations that passed through the evaluation indices, 2.0 °C, 2.5 °C, 3.0 °C, 3.5 °C, 4.0 °C and WBT were chosen to illustrate the spatial distribution of the discrimination results (Figs. 6 and 7). As shown in Fig. 6, the error percentage of snowfall days (*Ep*) was higher ($Ep > 10\%$) in the southeastern part of the basin and lower ($Ep < 10\%$) in the northern and western parts of the basin, which indicated high accuracies when identifying snowfall days in the northern and western parts of the basin and low accuracy in the southeastern part of basin. The areas with high *Ep* values ($Ep > 10\%$) increased as the temperature increased from 2.5 °C to 4.0 °C, which indicated that the *Ep* increased as the threshold temperature increased in the southeastern part of the basin when the threshold temperature excessed 2.5 °C. In addition, low *Ep* areas ($Ep < 10\%$) were most common at 2.5 °C and the WBT. Thus, 2.5 °C

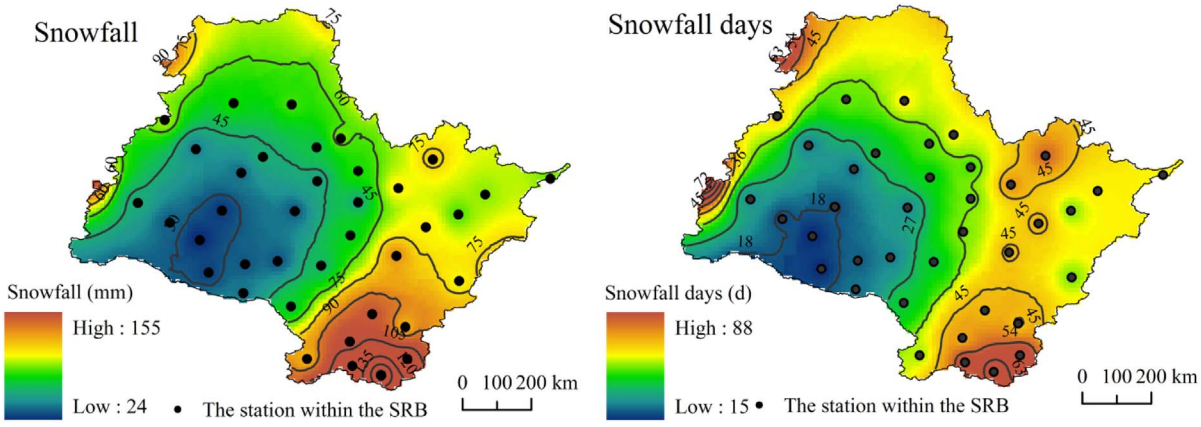

Fig. 2. Distribution of snowfall and snowfall days in the SRB during the period 1960–1979.

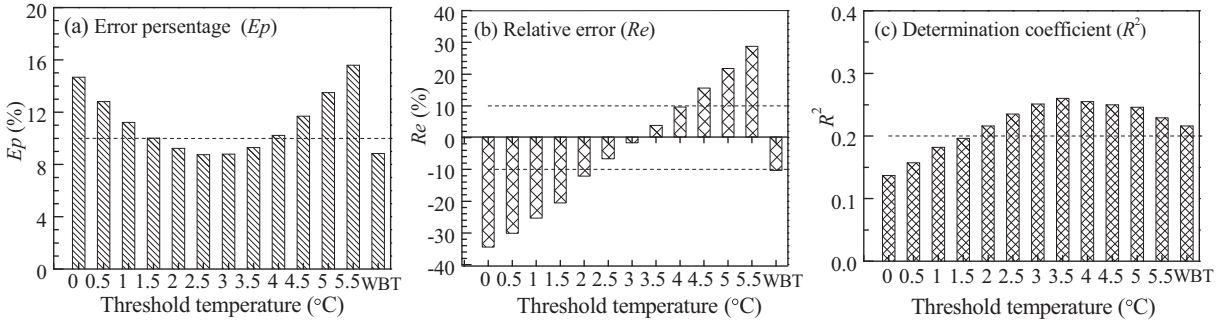

Fig. 4. Changes in the mean *Ep*, *Re* and R^2 at stations for different threshold temperatures in the SRB during the period 1960–1979.

and the WBT effectively discriminated snowfall days in most of the SRB.

As shown in Fig. 7, when the threshold temperatures were 2.0 °C, 2.5 °C and WBT, *Re* was below 0% at most stations, which indicated that snowfall was underestimated when the threshold temperature was 2.0 °C, 2.5 °C and WBT in most of the basin. When the threshold temperature increased from 2.0 °C to 4.0 °C, *Re* increased in the basin. Notably, *Re* was > 0% at most stations when the threshold temperature was 4.0 °C, indicating that snowfall was overestimated in the basin. In summary, snowfall was underestimated when the temperature threshold was the wet bulb temperature and when the temperature threshold was below 2.5 °C, whereas snowfall was overestimated when the temperature threshold exceeded 4.0 °C at most stations.

A comprehensive consideration of the spatial distribution discriminating results indicated high accuracy when identifying snowfall days in the northern and western parts of the basin, and low accuracy when identifying snowfall days in the southeastern part of the basin at the threshold temperatures. Snowfall was underestimated when the temperature threshold was the wet bulb temperature and when the temperature threshold was below 2.5 °C, whereas snowfall was overestimated when the temperature threshold exceeded 4.0 °C at most stations.

3.3. Identification and verification of the optimum temperature threshold at each station

3.3.1. Optimum temperature threshold at each station in the SRB

According to the discrimination results (*Ep*, *Re* and R^2) at the different temperature thresholds and the principles (Table 1) used to assess the optimum temperature in the SRB, the optimum thresholds for discriminating snowfall at different stations were confirmed (Fig. 8). As shown in Fig. 8, these optimum temperature thresholds varied at different stations. The optimum threshold temperatures were between 1.5 °C and 4.0 °C. Nineteen stations had an optimum threshold of 2.5 °C, the highest frequency among the stations, followed by 18 stations with a threshold of 3.5 °C, and 17 with a threshold of 3.0 °C. These three temperature thresholds accounted for the optimum thresholds at 54 stations, 90% of all stations. Two stations had optimum thresholds of 2.0 °C and 1.5 °C. However, 4 °C and WBT were the optimum thresholds for only 1 station each.

3.3.2. Discriminating snowfall based on the optimum temperature in the SRB

Using the optimum temperature thresholds at each station, the snowfall and snowfall days were separated from precipitation days between 1960 and 1979 in the SRB (Fig. 9). The discriminated snowfall days and snowfall were consistent with the observed snowfall days and snowfall in the SRB (Fig. 9). On average, there were 2.71 d of misclassified snowfall days annually, and *Ep* was 8.27% based on optimum temperature thresholds at each station; these values were lower than those of the single suitable temperature threshold at whole basin (2.86 d, 8.74% at 2.5 °C). Additionally, *Re* was −5.03%, which was lower than that of the single suitable temperature threshold in the entire basin (−6.66% at 2.5 °C). In comparison with the single temperature threshold used to discriminate snowfall in the entire basin, using the optimum temperature threshold at each station was more accurate.

Figs. 10 and 11 show the discriminated snowfall days and snowfall for 6 typical stations. The changes in discriminated snowfall and snowfall days were consistent with the observed snowfall and snowfall

Table 2
Changes in the discrimination results for different threshold temperatures in the SRB during the period 1960–1979.

Temperature threshold	Snowfall days				Snowfall			Heavy snow events
	Observed snowfall days	Identified snowfall days	Misclassified snowfall days	*Ep*	Observed snowfall	Identified snowfall	*Re*	R^2
0.0	32.73	28.63	4.80	14.68	52.09	34.13	−34.47	0.137
0.5	32.73	29.39	4.20	12.82	52.09	36.42	−30.09	0.157
1.0	32.73	30.12	3.67	11.21	52.09	38.91	−25.30	0.182
1.5	32.73	30.91	3.28	10.01	52.09	41.37	−20.58	0.196
2.0	32.73	31.69	3.02	**9.22***	52.09	45.77	−12.14	**0.216***
2.5	32.73	32.46	2.86	**8.74***	52.09	48.62	**−6.66***	**0.235***
3.0	32.73	33.20	2.88	**8.79***	52.09	51.26	**−1.59***	**0.251***
3.5	32.73	33.97	3.04	**9.28***	52.09	54.10	**3.85***	**0.260***
4.0	32.73	34.79	3.35	10.23	52.09	57.13	**9.68***	**0.255***
4.5	32.73	35.60	3.83	11.69	52.09	60.24	15.64	**0.250***
5.0	32.73	36.46	4.42	13.50	52.09	63.42	21.76	**0.246***
5.5	32.73	37.38	5.10	15.59	52.09	67.07	28.75	**0.229***
WBT	32.73	32.16	2.89	**8.82***	52.09	46.71	−10.34	**0.216***

Note: * and bold show denote the discriminated snowfall and snowfall days that met requirements of the given criteria (*Ep* < 10%, *Re* < 10% and R^2 > 0.2) and had a good effect when discriminating snowfall, snowfall days and heavy snowfall events.

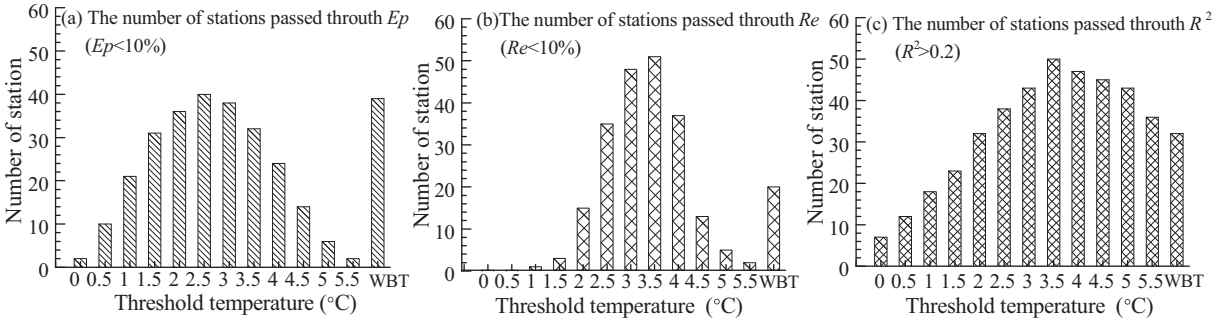

Fig. 5. Number of stations that satisfied the requirements of the evaluation indices.

days at the typical meteorological stations (Figs. 10 and 11). The annual mean numbers of misclassified snowfall days at stations 50136, 50745, 54266, 50632, 50854 and 54094 were 2.65 d, 1.80 d, 3.40 d, 2.65 d, 1.65 d and 3.5 d, respectively; the annual mean *Ep* values were 6.04%, 6.80%, 10.30%, 6.88%, 8.94% and 11.23%; and the annual mean *Re* values were −0.81%, 9.53%, −19.49%, −9.34%, −9.92% and −5.32%, respectively, for the corresponding six stations. Therefore, the optimum threshold at each station was able to effectively discriminate the number of snowfall days and snowfall from daily precipitation.

4. Discussion

Accurate snowfall discrimination is very important when researching hydrological processes and climate change at high latitudes and mountainous regions. This paper presented findings of snowfall discrimination in the SRB. The results showed that 2.5 °C was the optimum threshold temperature for discriminating snowfall in the entire basin. Due to the different landscape conditions of the different stations, the optimum temperature thresholds varied at different stations. The optimum thresholds at stations ranged from 1.5 °C to 4.0 °C. In comparison with the single temperature threshold, using an optimum temperature threshold for each station was more accurate when discriminating snowfall throughout the basin.

Some scholars have analysed suitable temperature thresholds in different regions throughout the world (USACE, 1956; Kienzle, 2008; Lauscher, 1982). For example, Auer (1974) analysed changes in the precipitation phase with temperature at 1000 surface weather stations in the United States and found that the probabilities of rain and snow were 50% at 2.2 °C, implying that a threshold temperature of 2.2 °C can be used to discriminate between snow and rain (Yang et al., 1997). Dai (2008) showed that snowfall mainly occurred at temperatures below 1.3 °C over land and below 2.3 °C over the ocean. Kienzle (2008) analysed the optimum threshold temperature at 15 stations in Canada and found that the optimum threshold temperatures range between 1.1 °C and 4.5 °C at each station and were mainly concentrated between 2.1 °C and 2.8 °C. Han et al. (2010) created a map of optimum temperature thresholds in China and found that the optimum thresholds were between 1.9 °C and 6.0 °C. According to these previous studies in different regions, the optimum threshold temperatures were between 0.5 °C and 6.0 °C and mainly concentrated between 1.1 °C and 4.5 °C. In this paper, we found that the optimum threshold temperatures of the stations in the SRB were between 1.5 °C and 4.0 °C, and 90% of the optimal

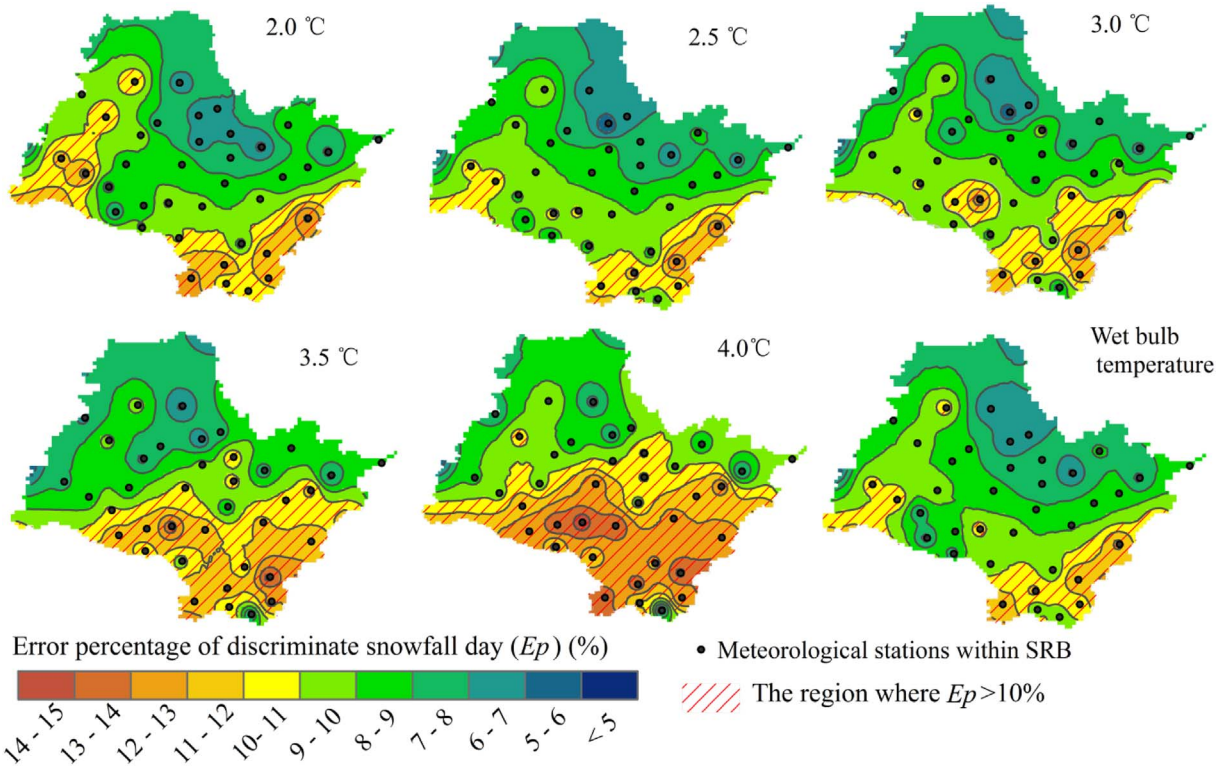

Fig. 6. Spatial distribution of the error percentage of discriminated snowfall days (*Ep*) for different threshold temperatures.

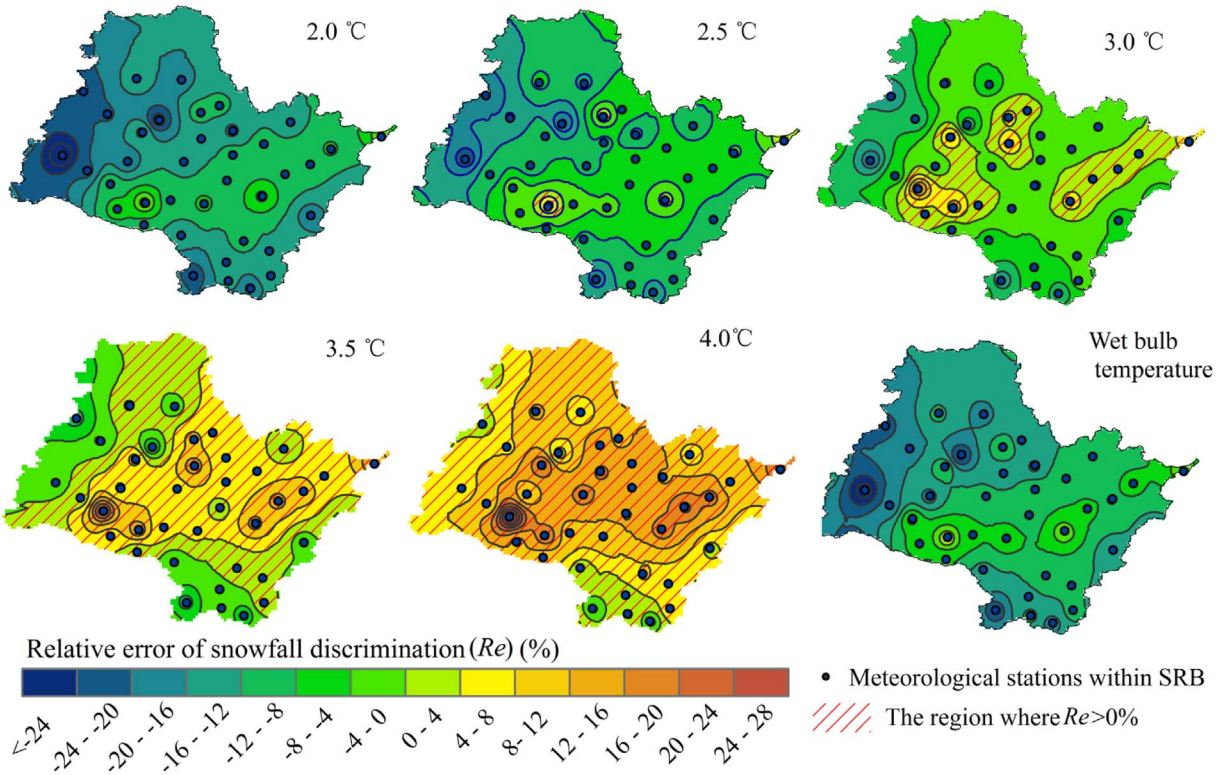

Fig. 7. Spatial distribution of the relative error of discriminated snowfall (*Re*) for different threshold temperatures in the SRB.

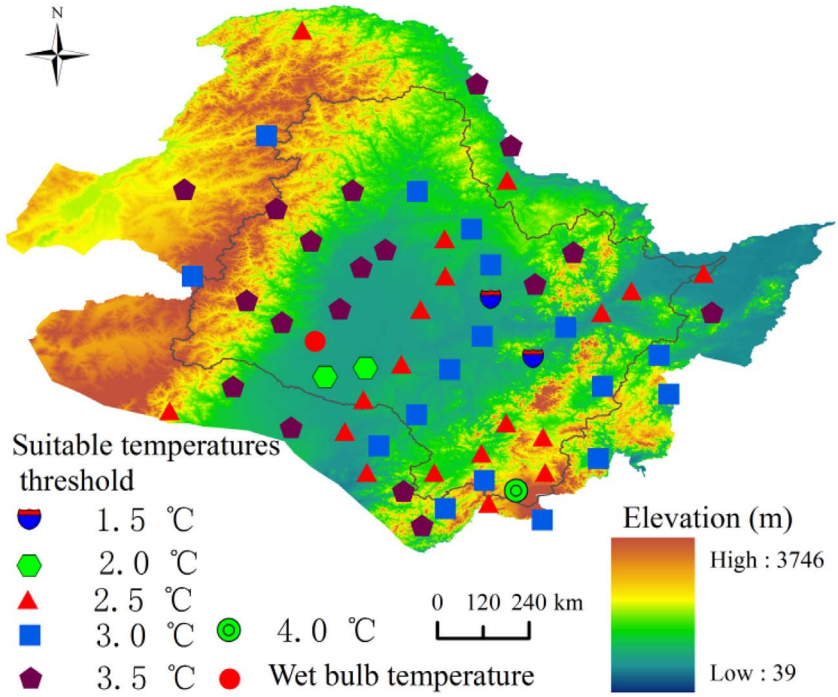

Fig. 8. Spatial distribution of the optimum threshold temperature in the SRB.

thresholds of stations were concentrated at 2.5 °C, 3.0 °C and 3.5 °C in the SRB. Thus, our results are similar to the findings of Auer (1974), Ye et al. (2013) and Ding et al. (2014).

The landscape condition is a critical factor that affects the temperature threshold. Some scholars have proposed that threshold temperatures were warmer at higher elevations. For example, Ding et al. (2014) demonstrated that the precipitation phase was highly dependent on the surface elevation and that high threshold temperatures were needed to differentiate between snow and rain in a high-elevation region. Chen et al. (2014) and Han et al. (2010) also observed a similar phenomenon in China. However, the phenomenon of high threshold temperatures at high elevations was not observed in this study. The lack of this phenomenon may be associated with the terrain in the SRB, which is dominated by plains and hills that account for 56.5% of the basin area. In addition, the highest station's elevation is 997.2 m, and the lowest is 66.4 m. Therefore, the elevation difference does not

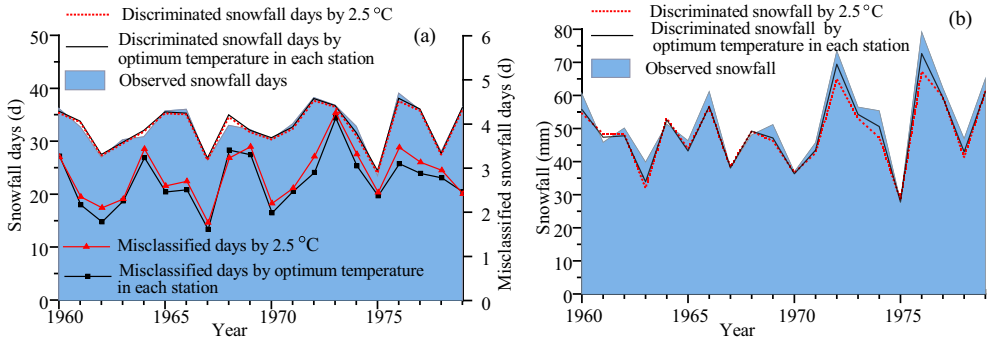

Fig. 9. Comparison of the discriminated snowfall days and snowfall based on the single temperature threshold and optimum temperature threshold at each station in the SRB from 1960 to 1979.

significantly affect changes in the threshold temperature. The distribution of threshold temperatures may also be affected by the evaluation index. In this paper, three indices (*Ep*, *Re* and R^2) were used to evaluate the discrimination accuracy and comprehensively identify the misclassified snowfall days, snowfall and heavy snowfall events. Optimum thresholds for each station were selected based on defined principles (Table 1), and these principles can affect the distribution of the optimum thresholds. In addition, the different optimum threshold temperatures of different stations may be related to differences in the relative humidity, wind speeds, air pressures and other atmospheric and landscape conditions at different stations (Kienzle, 2008; Ding et al., 2014; Harpold et al., 2017). However, these factors were not among this study's topics.

Ding et al. (2014) presented that WBT was a better indicator than air temperature for discriminating precipitation phases in China. In this study, the WBT was found to be capable of discriminating snowfall in the SRB (Table 2 and Fig. 6). However, it underestimated snowfall in the basin (Fig. 7). In addition, only one station's optimum threshold temperature was the WBT. Compared with temperatures of 2.5 °C, 3.0 °C and 3.5 °C, the WBT did not provide an obvious advantage. Chen et al. (2014) also found that the AT method performed better than the WBT method when the critical air temperature was 2.0 °C in China, which is consistent with the results of this study.

Zero degrees is a common threshold used to discriminate the precipitation phase (Kunkel et al., 2009; Qi and Fan, 2015; Rajagopal and Harpold, 2016). However, it underestimated 34.47% of snowfall in the SRB (Table 2), which was similar to the findings of Dai et al. (2008), Feiccabrino and Lundberg (2008), Ding et al. (2014), and Rajagopal and Harpold (2016). Some researchers used threshold temperatures without sufficient justification, and these temperatures were then used in further research, potentially resulting in uncertainty errors (Chen et al., 2016; Berghuijs et al., 2014). For example, Qi and Fan (2015) used 0 °C to estimate snowfall in the SRB and determined that the annual mean snowfall was 22.07 mm during 1960–2008, whereas the actual observed snowfall was 52.09 mm from 1960 to 1979, yielding a relative error of 57.63%. In this paper, 2.5 °C was determined to be the most suitable threshold temperature over the entire SRB, and the discriminated annual mean snowfall was 48.62 mm (a −6.66% relative

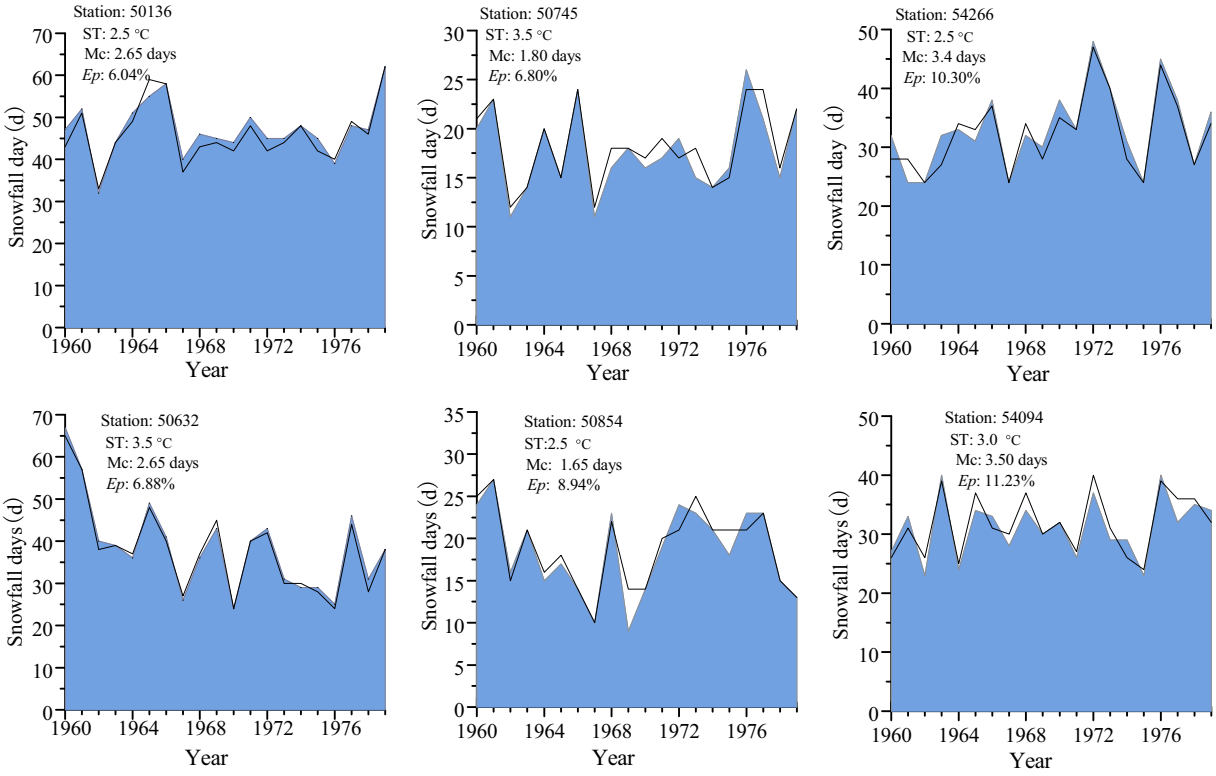

Fig. 10. Comparison of observed snowfall days and discriminated snowfall days based on the optimum temperature thresholds of typical stations.

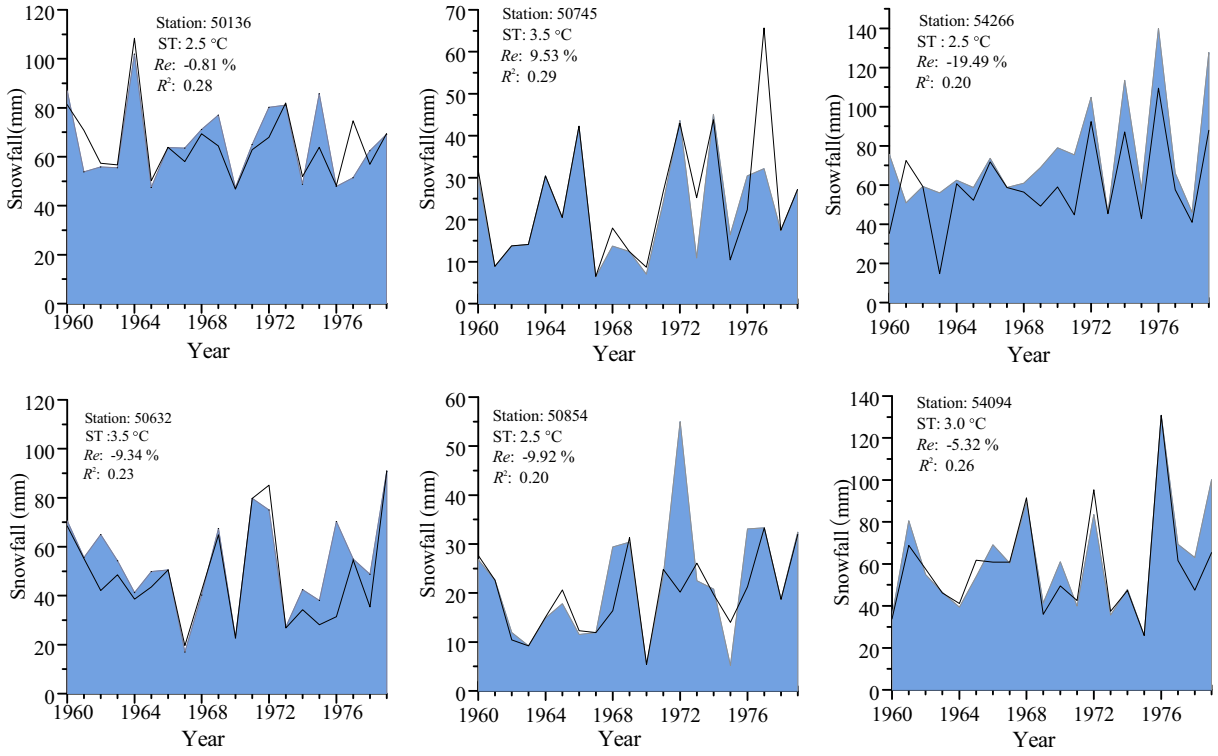

Fig. 11. Comparison of observed snowfall and discriminated snowfall based on the optimum temperature thresholds of typical stations.

error). Furthermore, it was more accurate to use the optimum threshold temperature at each station to discriminate snowfall (a −5.03% relative error) than a single suitable threshold temperature (2.5 °C). Therefore, it is necessary to confirm the optimum threshold temperatures in specific regions before using them; referencing the threshold temperatures in other regions or using 0 °C to discriminate the precipitation phase may result in uncertainties when analysing hydrological processes and climate change.

In this study, average air temperature was used to discriminate snowfall according to previous studies (Chen et al., 2014; Kienzle, 2008; Liu et al., 2016), and 2.5 °C was determined as the optimum threshold temperature for discriminating snowfall. Moreover, the minimum temperature and maximum temperature were also used to discriminate snowfall. For example, Rajagopal and Harpold (2016) found that optimum temperature threshold based on minimum temperature and maximum temperature showed more advantages than 0 °C of average air temperature in discriminating snowfall. Ruddell et al. (1990) established an empirical function between minimum temperature and type of precipitation observations, and found that minimum temperature could provide a more consistent relationship than that of average temperature (Schreider et al., 1997). Some snow models, such as Australian Snow Model (Schreider et al., 1997) and Regional Hydrological Simulation Systems Snow Model (Coughlan and Running, 1997), used a daily minimum air temperature scheme to estimate snowfall. In this study, six typical stations (Table 3) were selected to compare the differences by using average air temperature and minimum temperature through the temperature thresholds which were the above-mentioned. The results indicated that the optimum threshold temperature determined by daily minimum temperature was below than that determined by average air temperature in each station (Table 3). Moreover, the optimum temperature threshold in discriminating snowfall based on minimum temperature was near zero degree in each station. However, compared with the optimum temperature threshold in discriminating snowfall by average air temperature, discriminating the snowfall based on minimum temperature had higher error percentage (EP > 10%) in discriminating snowfall days.

Table 3
Optimum temperature thresholds and evaluation indices in discriminating snowfall based on average temperature and minimum temperature in the six typical stations.

Station number	Optimum temperature thresholds and evaluation indices (Ep, Re, R^2) for average temperature				Optimum temperature thresholds and evaluation indices (Ep, Re, R^2) for minimum temperature			
	OTT	Ep	Re	R^2	OTT	Ep	Re	R^2
50136	2.5 °C	6.04%	−0.81%	0.28	0.0 °C	14.95%	0.88%	0.12
50745	3.5 °C	6.80%	9.53%	0.29	0.0 °C	10.48%	2.08%	0.34
54266	2.5 °C	10.30%	−19.49%	0.20	0.5 °C	13.48%	8.73%	0.31
50632	3.5 °C	6.88%	−9.34%	0.23	0.0 °C	12.85%	−5.12%	0.22
50854	2.5 °C	8.94%	−9.92%	0.20	0.0 °C	14.09%	9.07%	0.23
54094	3.0 °C	11.24%	−5.53%	0.26	0.0 °C	17.65%	−4.58%	0.22

Note: OTT is optimum temperature threshold.

According to the evaluation indices and principles of selecting optimum temperature threshold (Table 1), there was higher accuracy for discriminating the snowfall based on optimum temperature threshold of average air temperature than that of minimum temperature.

The phases of precipitation are deeply influenced by the landscape conditions and meteorological conditions, such as temperature, wind speed, humidity and air pressure (Kienzle, 2008; Harpold et al., 2017). Precipitation and its phases are complicated processes (Liu et al., 2016). Discriminating snowfall based on one or two factors, such as air temperature and wet bulb temperature, without considering the physical mechanisms of snowfall will unavoidably cause errors when estimating snowfall. As a result, such discrimination schemes are incapable of being applied in real time and for emergency events such as floods and avalanches (Liu et al., 2016). However, such studies can provide critical parameters for discriminating precipitation events in hydrological and snow models, fill missing precipitation phase records, and provide scientific information for in-depth research on hydrologic processes and climate change in the SRB. In addition, in this study, snowfall was underestimated when the temperature threshold was the WBT and when the temperature threshold was below 2.5 °C, whereas snowfall

was overestimated when the temperature threshold exceeded 4.0 °C at most stations. These values provide reference information for discriminating precipitation events in other regions.

5. Conclusions

Thirteen temperature thresholds were used to discriminate snowfall in the SRB, and three evaluation indices (*Ep*, *Re* and R^2) were applied to evaluate the discrimination accuracy. The results showed that 2.5 °C was the optimum threshold temperature for discriminating snowfall on the scale of the entire basin. This value can provide a critical parameter when discriminating precipitation phases using hydrological and snow models at the basin scale.

Due to differences in the landscape conditions at different stations, the optimum thresholds varied. The optimal thresholds ranged from 1.5 °C to 4.0 °C. Optimal temperatures of 2.5 °C, 3 °C, and 3.5 °C were observed at 19 stations, 17 stations, and 18 stations, respectively, occupying 90% of the total number of stations in the basin. Compared with a single suitable temperature threshold for discriminating snowfall over the entire basin, it was more accurate to use the optimum threshold at each station to estimate the snowfall in the basin. These findings can be used to fill missing precipitation phase records in the SRB and provide scientific information for in-depth research on hydrological processes and climate change in the SRB.

In addition, snowfall was underestimated when the temperature threshold was the WBT and the temperature threshold was below 2.5 °C, whereas snowfall was overestimated when the temperature threshold exceeded 4.0 °C at most stations. These values also provide reference information for discriminating precipitation phases in other regions.

Acknowledgements

This study was financially supported by projects of National Key R& D Program of China (Grant No. 2016YFE0202900) and the National Natural Science Foundation of China (Grant No. 41571263).

Appendix A. Wet bulb temperature

Wet bulb temperature is the temperature of a parcel of saturated air if the saturation is due to evaporation into it, with the latent heat supplied by the parcel itself (Ding et al., 2014). Wet bulb temperature can be calculated as follows:

$$T_W = T - \frac{e_s(T)\cdot(1 - RH)}{0.000643P_a + \Delta}, \tag{A1}$$

where T_W is wet-bulb temperature (°C), T is air temperature (°C), RH is relative humidity and it ranges from 0 to 1, P_a is air pressure (hPa), $e_s(T)$ is the saturated vapor pressure (hPa) at T °C. $e_s(T)$ can be calculated by Tetens' empirical formula (Murray, 1967):

$$e_s(T) = 0.6108\cdot e^{17.27\cdot T/(T+273.2)}, \tag{A2}$$

T is air temperature (°C). Additionally, Δ can be calculated by equation:

$$\Delta = 4098\cdot e_s(T)\cdot(T + 237.2)^2, \tag{A3}$$

$e_s(T)$ is the saturated vapor pressure (hPa) at T temperature, and T is air temperature (°C).

References

An, J., Zheng, F., Wang, B., 2014. Using 137 Cs technique to investigate the spatial distribution of erosion and deposition regimes for a small catchment in the black soil region, Northeast China. Catena 123, 243–251. http://dx.doi.org/10.1016/j.catena.2014.08.009.

Arnold, J., Williams, J., Srinivasan, R., King, K., Griggs, R., 1994. Soil and Water Assessment Tool. US Department of Agriculture, Agricultural Research Service, Grassland, Soil and Water Research Laboratory, Temple, TX(For latest available SWAT version, see the SWAT website at: http://swat.tamu.edu/, Accessed: 20 April 2017).

Auer Jr., A.H., 1974. The rain versus snow threshold temperatures. Weatherwise 27, 67. https://doi.org/10.1080/00431672.1974.9931684.

Berghuijs, W.R., Woods, R.A., Hrachowitz, M., 2014. A precipitation shift from snow towards rain leads to a decrease in streamflow. Nat. Clim. Chang. 4, 583–586. http://dx.doi.org/10.1038/nclimate2246.

Bergström, S., 1992. The HBV Model: Its Structure and Applications. SMH1 Reports Hydrology No. 4 32 Swedish Meteorological and Hydrological Institute, S-60176 Norrköping, Sweden.

Bingner, R.L., Theurer, F.D., Yuan, Y., 2003. AnnAGNPS Technical Processes. USDA-ARS. National Sedimentation Laboratory. https://www.nrcs.usda.gov/wps/portal/nrcs/detailfull/national/water/quality/?&cid=stelprdb1043591, Accessed date: 20 April 2017.

Bourgouin, P., 2000. A method to determine precipitation types. Weather Forecast. 15, 583–592. http://dx.doi.org/10.1175/1520-0434(2000)015<0583:amtdpt>2.0.co;2.

Chen, R.S., Liu, J.F., Song, Y.X., 2014. Precipitation type estimation and validation in China. J. Mt. Sci. 11, 917–925. http://dx.doi.org/10.1007/s11629-012-2625-x.

Chen, Y., Li, W., Deng, H., Fang, G., Li, Z., 2016. Changes in Central Asia's water tower: past, present and future. Sci. Rep. 6, 35458. http://dx.doi.org/10.1038/srep35458.

Coughlan, J.C., Running, S.W., 1997. Regional ecosystem simulation: a general model for simulating snow accumulation and melt in mountainous terrain. Landsc. Ecol. 12 (3), 119–136.

Czys, R.R., Scott, R.W., Tang, K., Przybylinski, R.W., Sabones, M.E., 1996. A physically based, nondimensional parameter for discriminating between locations of freezing rain and ice pellets. Weather Forecast. 11, 591–598. http://dx.doi.org/10.1175/1520-0434(1996)011<0591:APBNPF>2.0.CO;2.

Dai, A., 2008. Temperature and pressure dependence of the rain-snow phase transition over land and ocean. Geophys. Res. Lett. 35, L12802. http://dx.doi.org/10.1029/2008gl033295.

Ding, B., Yang, K., Qin, J., Wang, L., Chen, Y., He, X., 2014. The dependence of precipitation types on surface elevation and meteorological conditions and its parameterization. J. Hydrol. 513, 154–163. http://dx.doi.org/10.1016/j.jhydrol.2014.03.038.

Fassnacht, S., Kouwen, N., Soulis, E., 2001. Surface temperature adjustments to improve weather radar representation of multi-temporal winter precipitation accumulations. J. Hydrol. 253, 148–168. http://dx.doi.org/10.1016/S0022-1694(01)00479-6.

Feiccabrino, J., Lundberg, A., 2008. Precipitation phase discrimination in Sweden. In: 65th Eastern Snow Conference. 2830. Fairlee, Vermont, USA.

Feiccabrino, J., Gustafsson, D., Lundberg, A., 2013. Surface-based precipitation phase determination methods in hydrological models. Hydrol. Res. 44 (1), 44–57. https://doi.org/10.2166/nh.2012.158.

Feng, X.Q., Zhang, G.X., Jun Xu, Y., 2013. Simulation of hydrological processes in the Zhalong wetland within a river basin, Northeast China. Hydrol. Earth Syst. Sci. 17, 2797–2807. http://dx.doi.org/10.5194/hess-17-2797-2013.

Guan, Y., Zheng, F., Zhang, X., Wang, B., 2017. Trends and variability of daily precipitation and extremes during 1960–2012 in the Yangtze River Basin, China. Int. J. Climatol. 37, 1282–1298. http://dx.doi.org/10.1002/joc.4776.

Habets, F., Boone, A., Champeaux, J.L., Etchevers, P., Franchisteguy, L., Leblois, E., Noilhan, J., Ledoux, E., Le Moigne, P., Martin, E., Morel, S., Noilhan, J., Quintana Seguı, P., Rousset-Regimbeau, F., Viennot, P., 2008. The SAFRAN-ISBA-MODCOU hydrometeorological model applied over France. J. Geophys. Res. 113 (D6), 304–312. http://dx.doi.org/10.1029/2007jd008548.

Han, C., Chen, R., Liu, J., Yang, Y., Qing, W., 2010. A discuss of the separating solid and liquid precipitations. J. Glaciol. Geocryol. 32 (2), 249–256 (in Chinese, with English Abstr.).

Harpold, A.A., Kaplan, M.L., Klos, P.Z., Link, T., McNamara, J.P., Rajagopal, S., Schumer, R., 2017. Rain or snow: hydrologic processes, observations, prediction, and research needs. Hydrol. Earth Syst. Sci. 21 (1), 1–22. http://dx.doi.org/10.5194/hess-21-1-2017.

Hock, R., 2003. Temperature index melt modelling in mountain areas. J. Hydrol. 282 (1), 104–115. http://dx.doi.org/10.1016/s0022-1694(03)00257-9.

Jiao, J., Xie, Y., Lin, Y., Chao, D., 2009. Study on snowmelt runoff and sediment yields in Northeast China. Geogr. Res. 28 (2), 333–344 (in Chinese, with English Abstr.).

Kienzle, S.W., 2008. A new temperature based method to separate rain and snow. Hydrol. Process. 22, 5067–5085. http://dx.doi.org/10.1002/hyp.7131.

Kunkel, K.E., Palecki, M.A., Ensor, L., Easterling, D., Hubbard, K.G., Robinson, D.,

Redmond, K., 2009. Trends in twentieth-century U.S. extreme snowfall seasons. J. Clim. 22, 6204–6216. http://dx.doi.org/10.1175/2009jcli2631.1.
Lauscher, F., 1982. Die Temperaturen der Termine mit Schneefall und Regen. Z. Angew. Meteorol. 34, 241–245.
Lin, B., Chen, X., Yao, H., Chen, Y., Liu, M., Gao, L., James, A., 2015. Analyses of land use change impacts on catchment runoff using different time indicators based on SWAT model. Ecol. Indic. 58, 55–63. http://dx.doi.org/10.1016/j.ecolind.2015.05.031.
Liu, S., Yan, D., Qin, T., Weng, B., Lu, Y., Dong, G., Gong, B., 2016. Precipitation phase separation schemes in the Naqu River basin, eastern Tibetan plateau. Theor. Appl. Climatol. http://dx.doi.org/10.1007/s00704-016-1967-7.
Lundquist, J.D., Neiman, P.J., Martner, B., White, A.B., Gottas, D.J., Ralph, F.M., 2008. Rain versus snow in the Sierra Nevada, California: comparing Doppler profiling radar and surface observations of melting level. J. Hydrometeorol. 9 (2), 194–211. http://dx.doi.org/10.1175/2007jhm853.1.
Marks, D., Winstral, A., Reba, M., Pomeroy, J., Kumar, M., 2013. An evaluation of methods for determining during-storm precipitation phase and the rain/snow transition elevation at the surface in a mountain basin. Adv. Water Resour. 55, 98–110. http://dx.doi.org/10.1016/j.advwatres.2012.11.012.
Maurer, E.P., Mass, C., 2006. Using radar data to partition precipitation into rain and snow in a hydrologic model. J. Hydrol. Eng. 11, 214–221. http://dx.doi.org/10.1061/(ASCE)1084-0699(2006)11:3(214.
Murray, F.W., 1967. On the computation of saturation vapor pressure. J. Appl. Meteorol. 6, 203–204. http://dx.doi.org/10.1175/1520-0450(1967)006<0203:otcosv>2.0.co;2.
Qi, F., Fan, H., 2015. Temporal-spatial distribution of snowfall in Songhua river basin. J. Arid Land Resour. Environ. 29 (6), 145–151 (in Chinese, with English Abstr.).
Qin, D., Shiyin, L., Peiji, L., 2006. Snow cover distribution, variability, and response to climate change in western China. J. Clim. 19, 1820–1833. http://dx.doi.org/10.1175/JCLI3694.1.
Rajagopal, S., Harpold, A.A., 2016. Testing and improving temperature thresholds for snow and rain prediction in the Western United States. J. Am. Water Resour. Assoc. 52 (5), 1142–1154. http://dx.doi.org/10.1111/1752-1688.12443.
Rauber, R.M., Olthoff, L.S., Ramamurthy, M.K., Kunkel, K.E., 2001. Further investigation of a physically based, nondimensional parameter for discriminating between locations of freezing rain and ice pellets. Weather Forecast. 16, 185–191. http://dx.doi.org/10.1175/1520-0434(2001)016<0185:FIOAPB>2.0.CO;2.
Ruddell, A.R., Budd, W.F., Smith, I.N., Keage, P.L., Jones, R., 1990. The southeast Australian alpine climate study. In: Report of the Department of Meteorology. 105 University of Melbourne, Victoria.
Schreider, S.Y., Whetton, P.H., Jakeman, A.J., Pittock, A.B., 1997. Runoff modelling for snow-affected catchments in the Australian alpine region, eastern Victoria. J. Hydrol. 200, 1–23.
Song, X., Song, S., Sun, W., Mu, X., Wang, S., Li, J., Li, Y., 2015. Recent changes in extreme precipitation and drought over the Songhua River Basin, China, during 1960–2013. Atmos. Res. 157, 137–152. http://dx.doi.org/10.1016/j.atmosres.2015.01.022.
Thériault, J.M., Stewart, R.E., Milbrandt, J.A., Yau, M.K., 2006. On the simulation of winter precipitation types. J. Geophys. Res. 111, D18202. http://dx.doi.org/10.1029/2005jd006665.
USACE, 1956. Snow Hydrology: Summary Report of the Snow Investigations. North Pacific Division, Portland OR.
Wang, J., Zhang, M., Wang, S., Ren, Z., Che, Y., Qiang, F., Qu, D., 2016. Decrease in snowfall/rainfall ratio in the Tibetan Plateau from 1961 to 2013. J. Geogr. Sci. 26 (9), 1277–1288. http://dx.doi.org/10.1007/s11442-016-1326-8.
Yang, Q., 2015. Study on Spatio-temporal Distribution of Snow Cover in Northeast China and Its Simulation on Snowmelt Runoff. Jilin University, Changchun, China (in Chinese, with English Abstr.).
Yang, Z.L., Dickinson, R.E., Robock, A., Vinnikov, K.Y., 1997. Validation of the snow submodel of the biosphere-atmosphere transfer scheme with Russian snow cover and meteorological observational data. J. Clim. 10, 353–373. http://dx.doi.org/10.1175/1520-0442(1997)010<0353:VOTSSO>2.0.CO;2.
Yang, W., Zheng, F., Han, Y., Wang, Z., Yi, Y., Feng, Z., 2016. Investigating spatial distribution of soil quality index and its impacts on corn yield in a cultivated catchment of the Chinese Mollisol Region. Soil Sci. Soc. Am. J. 80, 317–327. http://dx.doi.org/10.2136/sssaj2015.09.0335.
Ye, H., Cohen, J., Rawlins, M., 2013. Discrimination of solid from liquid precipitation over northern Eurasia using surface atmospheric conditions. J. Hydrometeorol. 14, 1345–1355. http://dx.doi.org/10.1175/JHM-D-12-0164.s1.
Zhang, A., Zhang, C., Fu, G., Wang, B., Bao, Z., Zheng, H., 2012. Assessments of impacts of climate change and human activities on runoff with SWAT for the Huifa River Basin, Northeast China. Water Resour. Manag. 26, 2199–2217. http://dx.doi.org/10.1007/s11269-012-0010-8.
Zhong, K., Zheng, F., 2017. Spatial and temporal variation characteristics of rainfall Erosivity in the Songhua River Basin from 1960 to 2014. J. Nat. Resour. 32, 278–291 (in Chinese, with English Abstr.).
Zhong, K., Chen, X., Chen, Y., Liu, M., 2016. Simulation of effects of topography and soil/land use spatial aggregation on sediment yield and runoff using AnnAGNPS. Trans. CSAE 32 (8), 127–135 (in Chinese, with English Abstr.).
Zhong, K., Zheng, F., Wu, H., Qin, C., Xu, X., 2017. Dynamic changes in temperature extremes and their association with atmospheric circulation patterns in the Songhua River Basin, China. Atmos. Res. 190, 77–88. http://dx.doi.org/10.1016/j.atmosres.2017.02.012.